J Biol Inorg Chem
DOI 10.1007/s00775-016-1435-y

MINIREVIEW

Photostable and photoswitching fluorescent dyes for super-resolution imaging

Masafumi Minoshima[1] · **Kazuya Kikuchi**[1,2]

Received: 28 October 2016 / Accepted: 28 December 2016

Abstract Super-resolution fluorescence microscopy is a recently developed imaging tool for biological researches. Several methods have been developed for detection of fluorescence signals from molecules in a subdiffraction-limited area, breaking the diffraction limit of the conventional optical microscopies and allowing visualization of detailed macromolecular structures in cells. As objectives are exposed to intense laser in the optical systems, fluorophores for super-resolution microscopy must be tolerated even under severe light irradiation conditions. The fluorophores must also be photoactivatable and photoswitchable for single-molecule localization-based super-resolution microscopy, because the number of active fluorophores must be controlled by light irradiation. This has led to growing interest in these properties in the development of fluorophores. In this mini-review, we focus on the development of photostable and photoswitching fluorescent dyes for super-resolution microscopy. We introduce recent efforts, including improvement of fluorophore photostability and control of photoswitching behaviors of fluorophores based on photochemical and photophysical processes. Understanding and manipulation of chemical reactions in excited fluorophores can develop highly photostable and efficiently photoswitchable fluorophores that are suitable for super-resolution imaging applications.

✉ Kazuya Kikuchi
kkikuchi@mls.eng.osaka-u.ac.jp

[1] Graduate School of Engineering, Osaka University, Suita, Osaka 565-0871, Japan

[2] Immunology Frontier Research Center (IFReC), Osaka University, Suita, Osaka 565-0871, Japan

Keywords Super-resolution microscopy · Fluorophores · Photostability · Photoactivation · Photoswitching

Introduction

Optical microscopy is a useful tool in biological research for the observation of biomolecules. In particular, fluorescence microscopy can visualize fluorescently labeled biomolecules with high contrast in cells and tissues using appropriate fluorophores, including fluorescent proteins [1], organic [2], and inorganic dyes [3]. Recently, super-resolution imaging has been developed as a set of new methods for overcoming the spatial resolution of the conventional light microscopy, which captures the detailed view of macromolecular complexes with better than 100 nm resolution in cells. In the previous two decades, several super-resolution imaging techniques have been developed that successfully acquire images in a subdiffraction area by exquisitely manipulating the fluorescence signals with optical setups [4, 5].

As fluorophores, organic fluorescent dyes are often utilized in super-resolution imaging because of their small size, bright fluorescence intensity, and high photostability. In most super-resolution microscopies, the use of typical fluorophores, such as fluorescent proteins, suffers from the rapid irreversible fading of the fluorescence (photobleaching) upon excitation with high laser intensity. Hence, fluorophores with excellent photostability are favored for long-term observation under harsh irradiation conditions. In addition, single-molecule localization-based super-resolution microscopy requires photoactivatable or photoswitchable fluorophores for irreversibly or reversibly changing the fluorescent properties under light irradiation. The control of fluorescence “on” and “off” states at a single-molecule

Published online: 12 January 2017

level enables precise localization of individual fluorescent molecules to obtain subdiffraction images. Since the aforementioned properties depend on photochemical reactions from excited fluorophores, understanding and control of photochemical processes of fluorescent molecules are essential for the use and development of fluorophores suitable for super-resolution imaging. In this mini-review, we introduce organic fluorescent dyes for super-resolution imaging by focusing on their photostability and photoswitching properties.

Spatial resolution of optical microscopy

The resolution limit of optical microscopy is defined as the shortest distance within which the image of two spots can be discriminated by the microscope system. When a light beam is focused on an object, the light wave creates blurred point-like objects, called the point spread function (PSF), because of the diffraction of light. The blurred distribution of the image is observed by integration with a real object via convolution processes. The resolution of the image can be improved by introducing a confocal system that optically removes out-of-focus signals and deconvolution processes that restore the blurring due to image convolution. Nevertheless, the resolution cannot be obtained below the distance (d) in the following Eq. (1) [6]:

$$d = \frac{\lambda}{2n\sin\theta}. \quad (1)$$

In the above equation, the resolution limit is determined based on the wavelength of the light (λ), the refractive index of the media (n) between the object and lens, and the angle of convergence (θ) of light. The $n\sin\theta$ term is known as the numerical aperture (NA) and it depends on the lens (a typical microscope has 1.4–1.6 NA). At visible wavelengths, the spatial resolution will be limited to 200–250 nm in the lateral axes. Within that range, the geometry of the fluorescence spots cannot be discriminated to observe a single blurred image (Fig. 1). As a result, it is difficult to find cellular macromolecular complexes or detailed structures with a size less than 100 nm owing to the limited image resolution of the conventional optical microscopies.

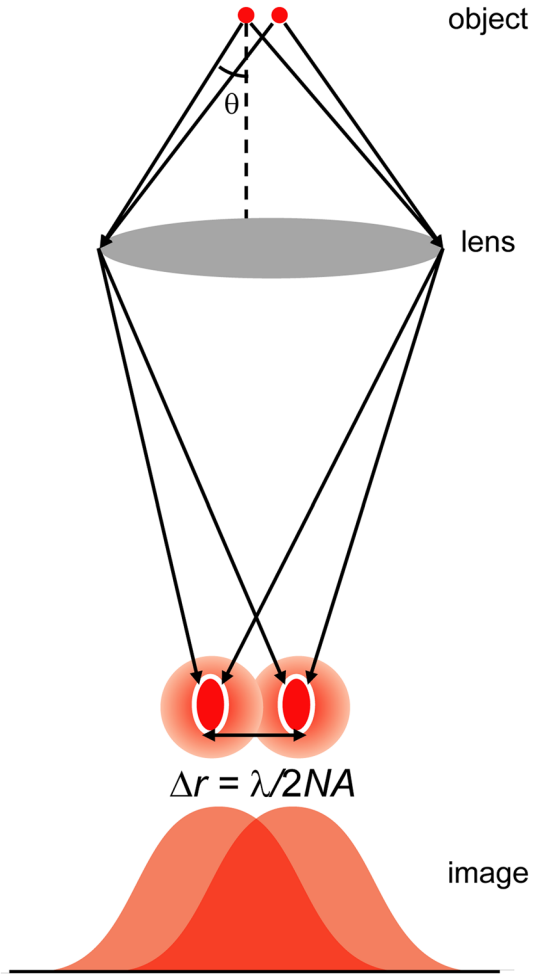

Fig. 1 Diffraction-limited image created by the optical setup of fluorescence microscopies. The fluorescence signals from the objects (*top*) create blurred spots (*bottom*), known as point spread functions though the lens. The minimum distance that can be discriminated between two spots is defined as the resolution limit (Δr), which can be determined by the wavelength and numerical aperture of the lens

Methods for super-resolution imaging

Super-resolution microscopy broke the diffraction barrier to allow imaging with improved resolution. Current super-resolution imaging methods can roughly be classified into two groups: (1) using patterned light illumination and (2) using single-molecule imaging. The first group includes stimulated emission depletion (STED) [7, 8] and the related methods reversible saturable optically linear fluorescence transitions (RESOLFT) [9] and saturated structured illumination microscopy (SSIM) [10]. In STED microscopy, some of the excited fluorophores are illuminated with an STED beam, a red-shifted light to induce forced transition of molecules from an excited, fluorescence "on" state to a ground, fluorescence "off" state. Typically, a ring-shaped STED beam illuminates the area containing excited fluorescent molecules. The STED beam depletes the fluorophores it illuminates before they spontaneously decay by fluorescence (Fig. 2). Thus, only the residual fluorescence in the center of the ring with a subdiffraction area is detected. An STED microscope can be set up by installing STED beams in a confocal scanning microscope system. The focal plane resolution (Δr) depends on the intensity of the STED beam, as shown in the following equation:

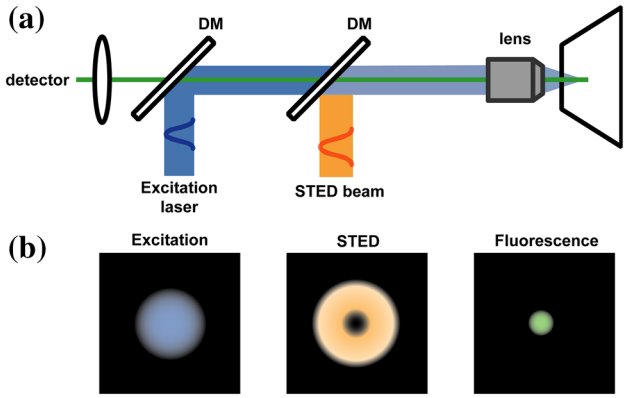

Fig. 2 **a** Illustration of the optical setup in STED microscopy. *DM* indicates dichroic mirror. Excitation and STED pulse lasers with ~ picosecond delay are irradiated to the object. The resultant fluorescence signal is collected by the detector. **b** Image spots by excitation laser (*left*), STED beam (*middle*), and fluorescence emission (*right*) in STED microscopy. The merged area of excitation and the ring-shaped STED causes loss of fluorescence signals due to the saturated transition to the dark (ground) state by the induced emission. The residual fluorescence in a small area is detected

$$\Delta r = \frac{\lambda}{2\mathrm{NA}\sqrt{1 + \frac{I\mathrm{max}}{I_\mathrm{s}}}}, \tag{2}$$

$I_{\max}$ represents the intensity of the laser depleting the fluorophore. I_s represents the saturation intensity, that is, the intensity required to induce depletion prior to competing transitions. From the above equation, subdiffraction resolution is achieved in the case of $I_{\max} \gg I_\mathrm{s}$. Under this condition, the saturated excited fluorophores undergo induced emission. Thus, the depleted area can be discerned as a region of negative contrast. Increasing the saturation intensity (the intensity of STED beam) results in higher resolution. Typically, STED allows subdiffraction imaging through the use of picosecond pulses of ~100 MW/cm^2 light irradiation as an STED beam.

Stimulated emission depletion has produced some valuable imaging successes. STED allowed subdiffraction images of protein clusters of synaptotagmin I on individual synaptic vesicles and revealed the function of clustering upon fusion of vesicles [11]. STED also enabled visualization of the assembled structures in viral particles [12], nuclear speckles [13], and lipid rafts [14]. Live-cell STED imaging has been reported for observing movement of dendritic spines in neuronal cells and uptake of viral particles in *Drosophila* larvae [15–17]. In principle, STED can be applied to in vivo super-resolution imaging [18], although phototoxicity may be an issue due to the intense laser irradiation.

Structured illumination microscopy (SIM) also enables subdiffraction imaging using patterned illumination techniques [19]. In this method, a morphological pattern of excitation light is created by interference of light beams. The resultant sample image reflects the sample structure itself depending on the excitation pattern (known as moiré fringes). Then, the reconstruction of multiple snapshots by scanning and rotating the patterned illumination provides subdiffraction images. Although the spatial resolution is limited (~100 nm) compared with other methods, the use of SSIM, that is, the nonlinear behavior of fluorophores upon saturated excitation, enables resolution below 100 nm [10]. The extension of three-dimensional scanning allows super-resolution imaging of the detailed structure of nuclear pore complexes [20]. SIM also allows time-lapse imaging in living cells using typical fluorophores. Super-resolution imaging was demonstrated to observe the dynamics of microtubules and kinesins in live cells with high temporal resolution with ~100 ms time frame [21].

Additional methods using single-molecule imaging include photoactivated localization microscopy (PALM) [22], stochastic reconstruction microscopy (STORM) [23], and other related methods. Single-molecule localization microscopy methods localize fluorophores at a single-molecule level (Fig. 3). Individual fluorescent molecules within the subdiffraction distance are stochastically excited, then the localization of the fluorophores is precisely determined by statistically fitting the detected spatial distribution of photons [24]. The resultant snapshots in each cycle are accumulated to reconstruct images. As the images are reconstructed from the localized fluorescence spots of each molecule, these methods achieve 20–30 nm spatial resolution (although the size of the fluorescent-labeled molecules limits the resolution). The resolution limit (σ, the deviation of spatial localization) of single-molecule localization microscopy can be defined with the following equation:

$$\sigma_{x,y}^2 \approx \frac{s^2 + a^2/12}{N} + \frac{4\sqrt{\pi}s^3b^2}{aN^2} \simeq \frac{s^2}{N^2}, \tag{3}$$

N denotes the number of photons. s, a, and b are the standard deviation of the PSF, the pixel size, and the mean background signal, respectively. As seen from the above equation, large numbers of photons from fluorophores and minimal background fluorescence achieve better spatial resolution. To reduce background fluorescence, total reflection illuminated fluorescence microscopy typically excitates a restricted area [25]. In addition, control of the number of active fluorophores in the objective area is critical, because simultaneous excitation of a large number of fluorescent molecules makes it impossible to discriminate the location of each fluorophore. To isolate fluorophores at a single-molecule level, photoactivatable or photoswitchable

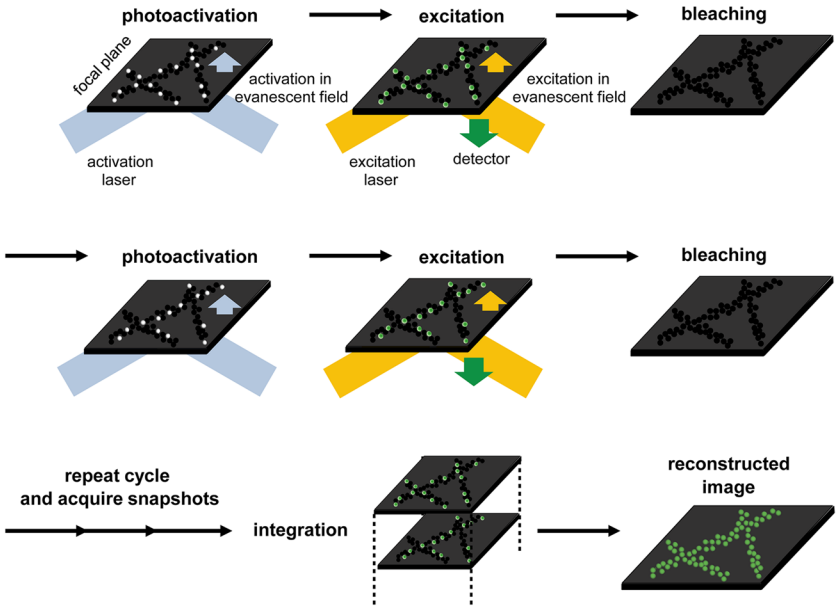

Fig. 3 Schematic illustration of the super-resolution imaging using single-molecule localization microscopy with a TIRF illumination system. Each cycle includes the photoactivation of a small set of fluorophores, excitation and detection of localization of activated fluorophores in the evanescent field, and bleaching. The reconstruction of each snapshot in the hundreds or thousands of repetitive operations provides the subdiffraction image

Table 1 Summary of super-resolution methods

	STED	RESOLFT	SIM	PALM/(d)STORM
Principle	Saturated transition	Saturated transition	Structured illumination	Single-molecule localization
Requirement of instrument	Two lasers for excitation and STED	Two lasers for excitation and photoswitching	Structured illumination	Near-field optics such as TIRF
Requirement of dyes	High photostability	Photoswitchable	None	Photoactivatable or photoswitchable
Lateral resolution	20–60 nm	50–100 nm	>100 nm	20–60 nm
Temporal resolution	0.035–10 s	0.5–10 s	0.1–1 s	0.5–30 min
Light intensity	0.1–1 GW/cm^2	1–80 kW/cm^2	5–30 W/cm^2	0.1–10 kW/cm^2
References	[7, 8, 12, 13, 15, 17, 18]	[9, 63]	[19]	[22, 23, 27, 73, 74, 79]

fluorophores are utilized, because the fluorescence properties are easily modulated by light irradiation [22, 23, 26]. A small number of the fluorophores are activated and selectively detected by fluorescence followed by photobleaching. The use of fluorophores with various colors, multicolor PALM or STORM imaging, has demonstrated the ability to reveal detailed macromolecular complexes of microtubules and clathrin-coated pits in cells, colocalization of different protein pairs in cell adhesion complexes, and interactions in organelles or cytoskeletons [27–31]. STORM also imaged detailed localization of specific genomic regions in chromosome, which revealed chromatin organization by interaction between topologically associating domains and chromatin folding in different epigenetic states [32, 33]. PALM and STORM were also applied to live-cell super-resolution imaging [27, 34]. However, integration of the hundreds of snapshots takes time to obtain reconstructed images, which limits the temporal resolution of live-cell super-resolution imaging.

The characteristics of the representative super-resolution methods are summarized in Table 1. As shown in the table, each method has different properties with regard to spatial resolution, temporal resolution, and limitations. For example, STED microscopy visualizes images with high spatiotemporal resolution (20–60 nm); however, it has limitations in the application to live-cell imaging due to the phototoxicity of the samples and photobleaching of fluorophores. RESOLFT, a modified method of STED, can reduce the light intensity to allow live-cell imaging applications; however, the spatiotemporal resolution is slightly lower than that of STED. In addition, the super-resolution microscopies have intrinsic tradeoffs between spatial and temporal resolutions, particularly found in structured illumination and single-molecule localization microscopies. For example, SIM has a higher temporal resolution (0.1–1 s) in spite of lower spatial resolution (~100 nm). Single-molecule localization approaches, such as PALM and (d)STORM, realize high spatial resolutions

(20–60 nm) and are easy to expand to multicolor imaging; however, such methods have significantly lower temporal resolution (0.5–30 min), resulting in difficulties to conduct live-cell imaging applications. Furthermore, the light intensity in super-resolution microscopies is higher than that in the conventional fluorescence microscopies which largely limit the choice of fluorophores. This will be discussed in detail in the following section.

Requirement of photostability for super-resolution imaging

In most cases of super-resolution imaging, stability of the fluorophores under continuous light irradiation is essential. In particular, STED microscopy uses a laser with extremely high intensity (~100 MW/cm^2) to reach subdiffraction resolution. The intensity of the STED beam is much higher (on the order of 10^6–10^7 magnitudes) than that of the excitation light sources of the conventional confocal laser fluorescence microscopy. Therefore, fluorophores must be stable under the severe illumination conditions of STED imaging. As fluorescent proteins are still limited to use because of fast photobleaching [35], researchers prefer to use organic fluorophores with high photostability, such as rhodamine derivatives, and inorganic luminescent semiconductors, such as quantum dots. For labeling of specific biomolecules, antibody-dye conjugates are employed in STED. For single-molecule localization-based microscopies, such as PALM and STORM, highly photostable fluorophores are also desired to obtain good fluorescence contrast of single molecules. Rapid inactivation of fluorophores limits the ability to gain enough photons to distinguish fluorophores from the background.

Photostability can be evaluated by ensemble and single-molecule systems. For ensemble systems, a bulk solution of fluorophores is irradiated by a laser with the desired intensity and wavelength characteristics for use in imaging applications. The residual fluorescence is measured and plotted at each timepoint after irradiation. As a light source and a fluorescence spectrometer are required for the experiment, this is a facile method to evaluate photostability of fluorophores. On the other hand, the single-molecule system detects photons emitted from each fluorophore immobilized on a substrate after exposure to an excitation laser. The photostability of the fluorophore is evaluated by the duration of detected photon counts from an individual fluorophore. The result directly reflects single-molecule imaging-based applications, including super-resolution microscopy.

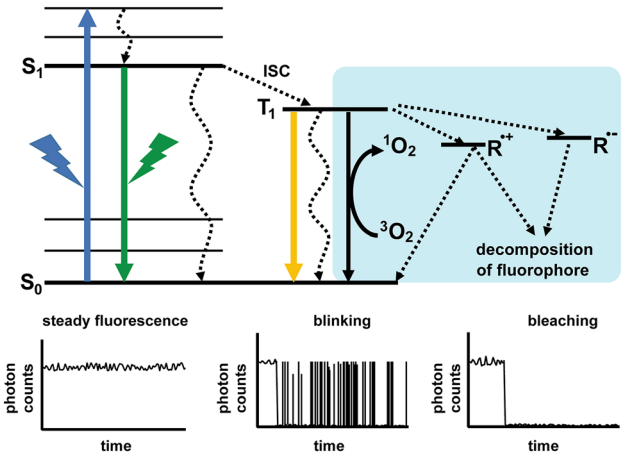

Fig. 4 Photochemical processes of the excited fluorophores. Blue, green, and yellow arrows represent excitation, emission in fluorescence, and emission in phosphorescence, respectively. The curved arrows indicate internal conversion. Fluorophores in triplet states can undergo redox reactions to produce radical cations ($R^{\cdot+}$) and anions ($R^{\cdot-}$) or reaction with oxygen to produce singlet oxygen ($^1O_2$) and reactive oxygen species, resulting in decomposition of the chemical structure. The three graphs at the bottom are time-dependent detected photon counts of the single fluorophores in steady fluorescence (*left*), fluorescence blinking (*middle*), and bleaching (*right*)

Photobleaching mechanism of fluorophores

Photochemical processes upon excitation are highly involved in the photostability of fluorophores (Fig. 4) [36, 37]. When fluorophores are excited from the ground state (S_0) by light irradiation, the excited fluorophores immediately undergo relaxation to the lowest vibrational energy level of the singlet electronic excited state (S_1). The fluorophores in the S_1 state can go back to the S_0 state with radiative (fluorescence) or nonradiative (internal conversion) pathways, or transition to a triplet state (T_1) by intersystem crossing. While the transition to T_1 rarely takes place in typical fluorophores, fluorophores in T_1 have a relatively longer lifetime (10^{-4} to $^{-6}$ s). In particular, oxygen is a significant reactive molecule against fluorophores in the T_1 state under ambient conditions. The one-electron transfer reaction from the triplet state molecules to molecular oxygen produces a superoxide radical anion ($O_2^{\cdot-}$) and a radial cation of the fluorophores ($F^{\cdot+}$). In addition, energy transfer from T_1 fluorophores produces singlet oxygen ($^1O_2$). Such reactive oxygen species (ROS) may disrupt the structure of the fluorophore, resulting in conversion of the fluorophore to permanent nonfluorescent decomposed products (photobleaching).

Development of highly photostable fluorophores

As described in the previous section, the photobleaching process is associated with the chemical reactions between excited fluorophores in the T_1 state and surrounding molecules, mediated by electron or energy transfer. Hence, inhibition of the reactions mediated by the T_1 state is a rational way to improve photostability of fluorophores. Depletion of oxygen in the media by N_2 bubbling is the first strategy for suppression of chemical reactions associated with ROS. A combination of glucose with glucose oxidase and catalase is also utilized to enzymatically consume oxygen in buffer [38]. These methods can reduce the probability of collision between triplet state fluorophores and molecular oxygen to elongate the fluorescence duration time.

An alternative strategy is encapsulation of fluorophores with host molecules to hinder the access of molecular oxygen. In a hydrophobic environment of host molecules, fluorophores are also protected from water molecules that can cause reactions of excited fluorophores. Encapsulation of the rhodamine 6G fluorophore with cucurbit [7] uril as a supramolecular host largely enhanced its photostability, and the complex could be applied to single-molecule imaging [39, 40]. Improvement of photostability of a cyanine dye Cy5 was also reported by encapsulation with a cyclodextrin host molecule [41]. Yang et al. demonstrated suppression of photobleaching and photoblinking of a hydrophobic borondipyrromethene (BODIPY) derivative by linking with hydrophilic polyglycerol dendrimers that serve as a protective moiety [42].

In addition, photostability of some fluorophores can be improved by modification of their chemical structures. The introduction of electron-withdrawing substituents, such as carbonyl, sulfonyl, nitrile, and fluorine groups, lowers the lowest unoccupied molecular orbital (LUMO) levels of the molecules. Since the energy level of the triplet state is also lowered, the reactivity against molecular oxygen and singlet oxygen is suppressed. This strategy has been employed to develop photostable fluorophores of BODIPYs, cyanines, and xanthenes [43–46]. Grimm et al. recently reported a method to improve photostability by locking of *N*,*N*-dialkylamino groups in the fluorophores to inhibit the nonemissive twisted internal charge transfer (TICT) state upon excitation [47]. The TICT state can have diradical intermediates via intramolecular electron transfer, which may result in permanent bleaching [48]. Then, *N*,*N*-dialkyl groups of coumarin, rhodamine, and oxazine derivatives were replaced with azetidines [47]. The interlocked fluorophores significantly improved not only the photostabilities but also the fluorescence quantum yields. The improved fluorophore conjugates were applied to STORM super-resolution imaging of the nucleus.

Stabilization of fluorophores by triplet state quenchers

Photobleaching of fluorophores is also suppressed by addition of the redox-active molecules, such as beta-mercaptoethanol (β-ME), mercaptoethylamine (MEA) 6-hydroxy-2,5-,7,8-tetramethylchroman-2-carboxylic acid (Trolox), *n*-propylgallate, ascorbic acid, and 4-nitrobenxzyl alcohol (NBA). These molecules, known as triplet state quenchers, can quench the reactive triplet state fluorophores via electron transfer before reaction with molecular oxygen (Fig. 5) [49–51]. Cyclooctatetraene (COT) is also used as a triplet state quencher, because it quenches singlet oxygen via energy transfer. The co-incubation of these triplet state quenchers with the fluorophores significantly enhanced the fluorescence duration time without rapid photobleaching or photoblinking in single-molecule imaging [52, 53]. Moreover, Vogelsang et al. reported considerable improvement of the photostability by simultaneous use of reductant and oxidant in single-molecule imaging [54]. The fluorescence duration times of the fluorophores ATTO647N and Cy5 dyes were increased in the presence of ascorbic acid as a reductant and methyl viologen (MV) as an oxidant in single-molecule imaging analysis. They mentioned the plausible mechanism that the fluorophore in the T_1 state is reduced by the reductant following oxidation to reproduce the ground state, which can be explained by the energy levels and the redox potentials of each molecule. Thus, the combinatorial use of reductants and oxidants is a useful method for suppression of photoblinking and photobleaching of fluorophores to obtain a better image quality in super-resolution imaging. However, one may be concerned about the effects of the redox-active triplet state quenchers on physiological systems in live cells, because a high concentration (over millimolar concentrations) of them is needed for improvement of photostability.

Among the transition metal ions, nickel (Ni^{2+}) has been known as a triplet state quencher of various organic chromophores [55]. Glembockyte et al. demonstrated that Ni^{2+} can be used to enhance photostability of a Cy3 dye in a single-molecule imaging experiment using an immobilized Cy3-labeled DNA duplex in Ni^{2+}-containing buffer (Fig. 6a) [56]. Further analysis revealed that the enhancement of photostability is attributed to physical quenching of the triplet state via energy transfer. While other triplet state quenchers require concentrations higher than millimolar ranges (2 mM Trolox and 143 mM β-mercaptoethanol) to improve the photostability, Ni^{2+} suppressed the fluorescence bleaching at submillimolar concentrations (0.1 mM).

Furthermore, hybrid fluorophores directly linked with triplet state quenchers were developed to decrease the concentration of triplet state quenchers (Fig. 6b). Altman et al.

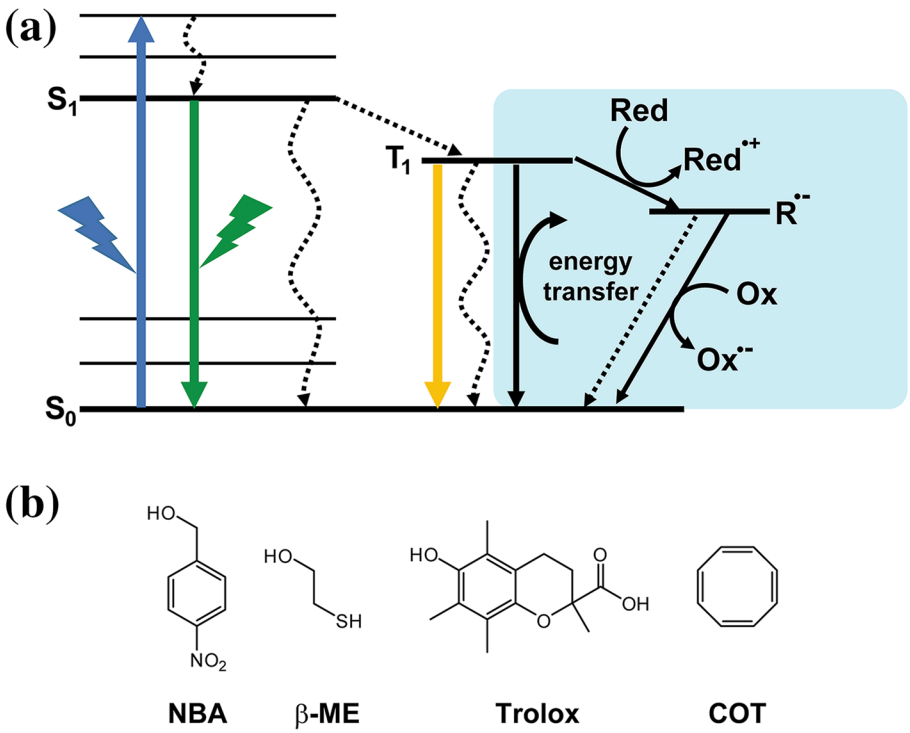

Fig. 5 **a** Schematic diagram of the roles in triplet state quenchers. Redox-active molecules can react with the triplet state of the excited fluorophores to produce their radical anions ($R^{\cdot-}$) following oxidation and transfer to the ground state. Fluorophores in the triplet state are also relaxed to the ground state via energy transfer by a quencher, such as COT. **b** Chemical structures of the triplet state quencher molecules for stabilization of the fluorophores

investigated the effect of distance between triplet state quenchers and Cy5 fluorophores on photostability [57]. They tethered triplet state quenchers (COT, Trolox, and NBA) and Cy5 in DNA strands with different geometries to alter the distance. A single-molecule imaging experiment revealed enhancement of fluorescence stability by triplet state quenchers in a distance-dependent manner. Based on this finding, highly photostable fluorophores are developed by directly tethering cyanine fluorophores with the aforementioned triplet state quenchers (Fig. 6c) [58]. Such fluorophore conjugates showed improved photostability without the addition of an excess amount of triplet state quencher. In these conjugates, the T_1 quenching effects intramolecularly occur from the proximately positioned triplet state quenchers via electron or energy transfer [59, 60]. Such self-healing dyes are available for single-molecule and super-resolution imaging applications. Van der Valde et al. recently developed a conjugate of KK114 (a rhodamine derivative) directly linked with NBA as a triplet state quencher and demonstrated immunolabeling with the fluorescent dye for STED imaging of nuclear pore complexes (Fig. 6c) [61]. Although the efficiency of triplet quenching effects depends on the combination of triplet state quencher molecules and fluorophores, the use of triplet state quenchers is a useful method for observation of biomolecules in super-resolution microscopies.

Photoswitching property in super-resolution microscopy

Photoactivation or photoswitching properties are key for single-molecule localization-based super-resolution microscopy. PALM uses photoactivatable fluorophores that irreversibly turn on fluorescence, while STORM uses photoswitchable fluorophores that reversibly transition between fluorescence emissive and nonemissive states. In both methods, the small number of fluorophores in the diffraction-limited area can be detected upon activation by irradiation with excitation light of distinct wavelengths. In addition, an STED-related method, RESOLFT, uses photoswitchable fluorophores for the saturated transition to a nonemissive state by illumination with a patterned shape [62, 63]. Compared with STED microscopy, RESOLFT can reduce the light intensity for saturated photoswitching of fluorophores, which can be suitable for cellular imaging applications [64, 65]. Whereas photoactivatable and photoswitchable fluorescent proteins are available for these super-resolution imaging methods, organic fluorophores are also utilized because of their high brightness. For single-molecule analysis, it is important to precisely detect the localization of the fluorescence signals from each fluorophore.

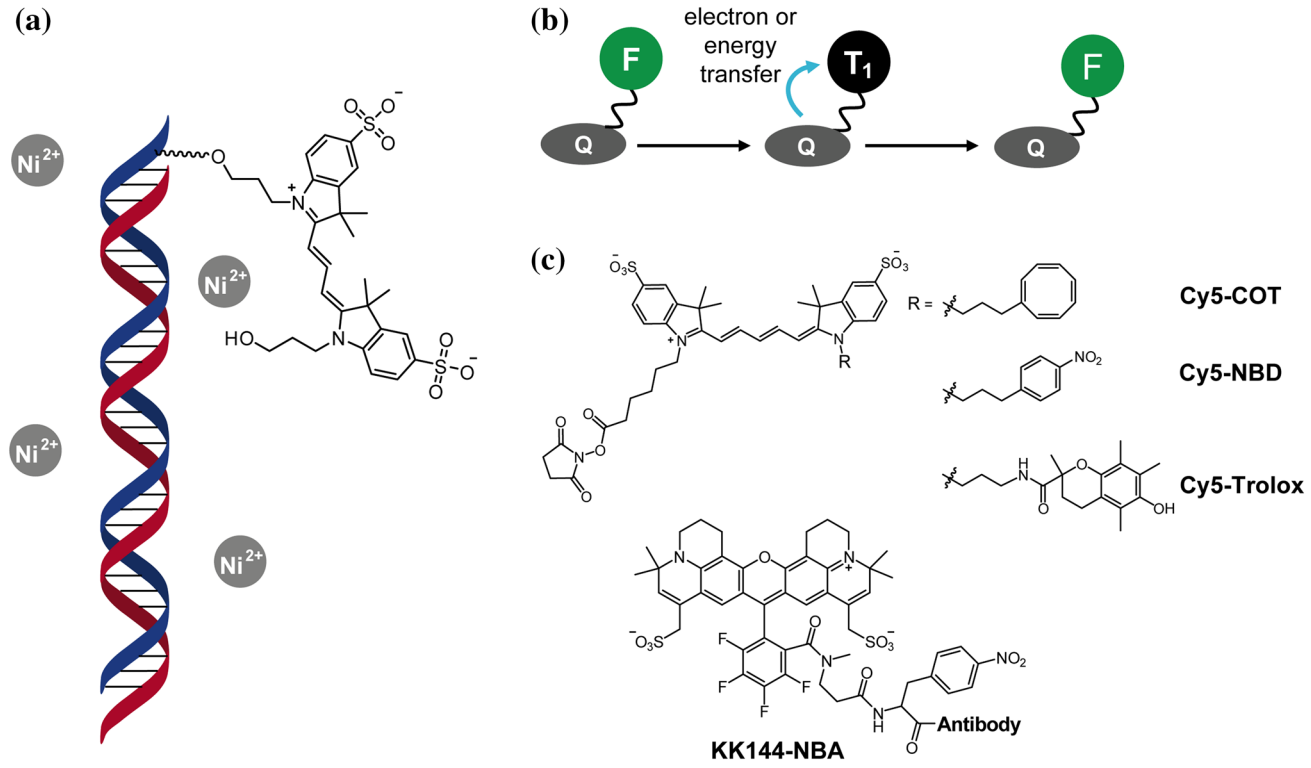

Fig. 6 **a** Stabilization of Cy3 fluorophores (conjugated in the DNA) by nickel ions. **b** Schematic illustration of self-healing fluorophores by conjugation of triplet state quencher (Q) with fluorophore (F). Fluorophore in triplet state (T_1) is recovered to its ground state by electron or energy transfer from the proximal triplet state quencher. **c** Chemical structures of the reported self-healing fluorescent probes (Cy5 and KK144 conjugates)

Photoactivatable fluorophores

For PALM imaging, photoactivatable fluorophores bearing photolabile protecting (caging) groups have been developed [66, 67]. Typical caging groups, such as *o*-nitrobenzyl and coumarinyl groups, are efficiently removed by UV light irradiation. Introduction of caging groups into appropriate positions of fluorophores, such as fluoresceins, rhodamines, and other fluorophores inactivates their fluorescence (Fig. 7a) [68]. After UV illumination with controlled light intensity, a small set of fluorophores is activated and imaged to obtain subdiffraction images. In terms of high photostability, caged rhodamine derivatives are utilized for super-resolution imaging by PALM. Wysocki et al. reported a facile synthetic method of producing caged xanthene dyes, including rhodamine and Si-rhodamine derivatives (Fig. 7b) [69, 70]. In the synthetic scheme, a reduced form of rhodamines (*leuco*-rhodamines) allows more efficient installation of caging groups to the fluorophores under mild conditions. They demonstrated PALM imaging using the developed caged fluorophores and mentioned the possibility of multicolor imaging using different caged rhodamine derivatives. Belov et al. developed a different class of caged rhodamines by transforming a carboxy group into a 2-diazoketone group (Fig. 7b) [71]. Introduction of 2-diazoketone group allows formation of a nonfluorescent, ring-closed structure. Under UV irradiation, elimination of N_2 and subsequent Wolff rearrangement produces a fluorescent form of rhodamine along with a nonfluorescent minor product. This dye was used in monochromatic multilabel super-resolution imaging in combination with another photoactivatable rhodamine dye with different activation wavelengths. Moerner's group also reported a caged derivative of a push–pull type fluorophore, dicyanomethylenedihydrofuran, by replacing an amine group with a photolabile azide group to modulate optical properties of the fluorophore (Fig. 7b) [72]. Upon irradiation with blue light, the azide-to-amine reduction of the fluorophore significantly increased the red fluorescence emission, which can be utilized for super-resolution imaging in mammalian cells.

Photoswitchable fluorescent dyes

Stochastic reconstruction microscopy requires photoswitchable fluorophores to achieve super-resolution imaging (Fig. 8a). Early study by Zhuang's group demonstrated

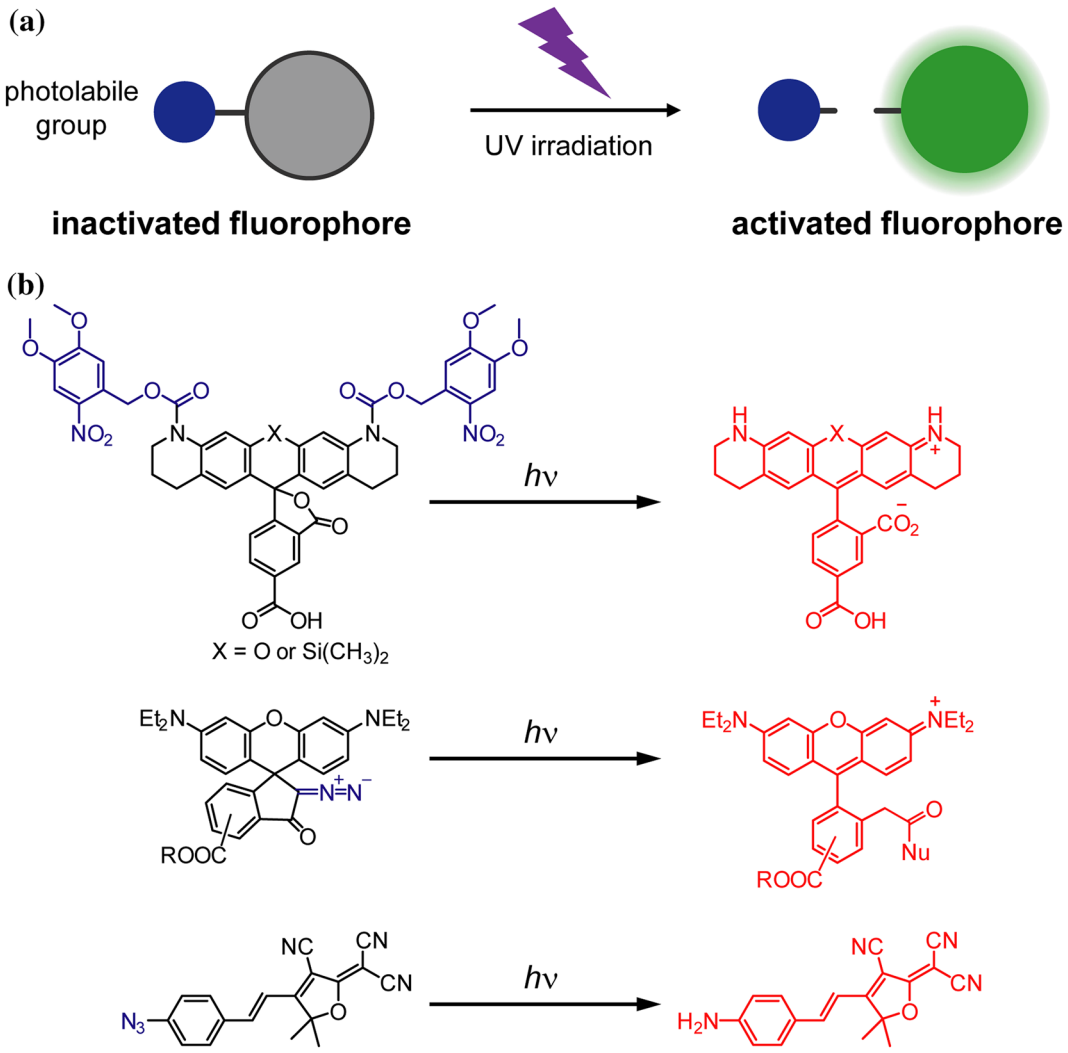

Fig. 7 **a** Schematic illustration of photoactivation of fluorophores by light irradiation. **b** Chemical structures of caged (inactivated) and uncaged (activated) fluorophores for single-molecule localization super-resolution microscopy. The photolabile groups are shown in *blue*

single-molecule imaging by photoswitching via interaction between a pair of cyanine dyes (Cy3 and Cy5) at proximal positions by tethering to each strand of double-stranded DNA [73]. Irradiation of red light corresponding to Cy5 absorption results in a large fluorescence decrease, indicating the transition to fluorescence off states. Whereas green light irradiation corresponding to the absorption of Cy3 recovered the Cy5 fluorescence, indicating the re-activation of Cy5 fluorescence by excitation of the proximal Cy3. This photoswitching cycle between "on" and "off" can be repeated until photobleaching occurs. The STORM principle can be used in many organic and protein-based fluorophores and applied to multicolor super-resolution imaging in combination with different pairs of fluorophores, an emitting fluorophore and an activating fluorophore [23, 30, 73]. In addition, Sauer et al. reported modified STORM imaging to acquire subdiffraction fluorescence images using a single fluorophore, called directed STORM (dSTORM) [74]. In this method, single fluorophores can be reversibly photoswitched between on and off states without the use of an activating fluorophore. Such photoswitching behaviors are found in a variety of the conventional fluorophores, including cyanines, oxazines, and rhodamines in appropriate conditions of reductants and their concentrations, pH, and oxygen concentration in buffer (Fig. 8b) [75, 76]. The fluorescence reduction is induced by the transition to the nonfluorescent intermediates bearing relatively longer lifetimes by chemical reactions of the excited fluorophores (Fig. 8a). In the case of cyanine fluorophores, the excited molecules can react with nucleophilic thiols to produce thermally stable adducts at polymethine chain moieties even in the presence of oxygen (Fig. 8c) [77]. The adducts are nonfluorescent and can be activated with light irradiation. Several fluorophores also react with

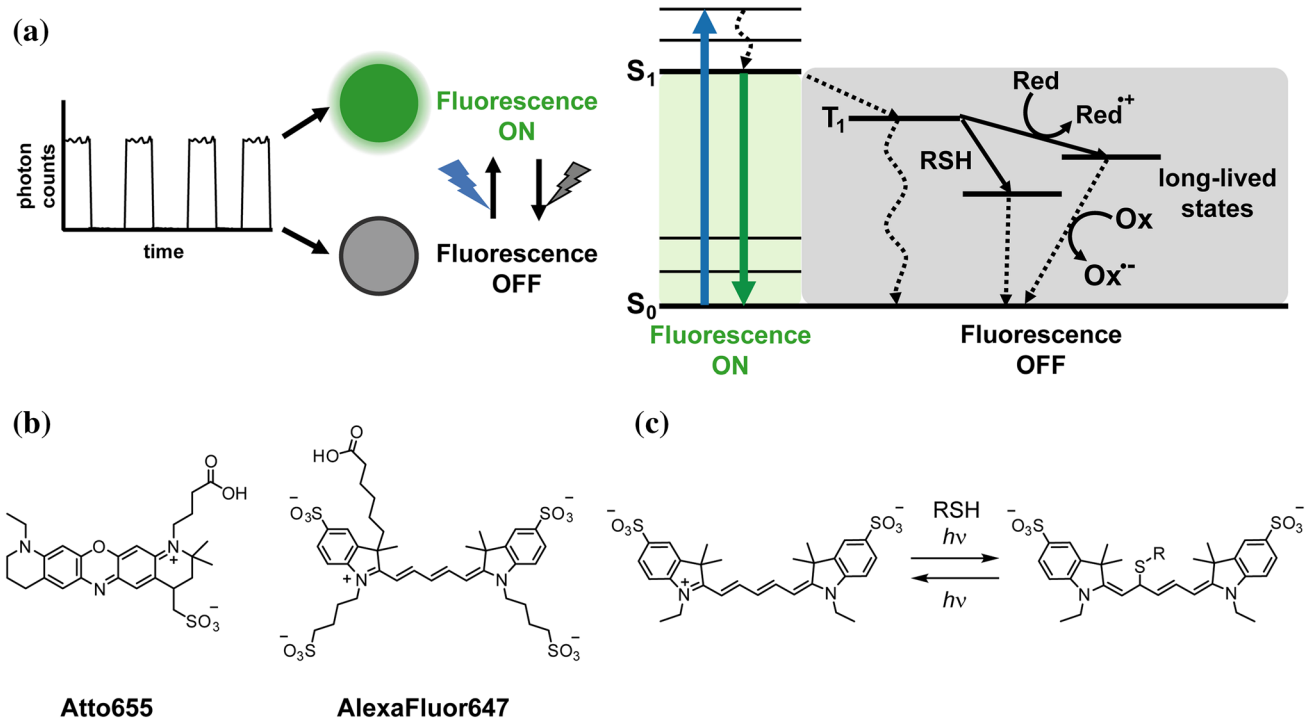

Fig. 8 **a** Schematic illustration of photoswitching of fluorophores (*left*) and the photochemical processes of photoswitching between fluorescence ON and OFF states (*right*). Transition to the long-lived and nonemissive states causes switching behaviors in fluorescence. The addition of thiols, reductants, and oxidants helps fast recovery of the fluorophores before photobleaching. **b** Chemical structures of the photoswitchable fluorophores used for STORM and dSTORM. **c** Photoswitching property of Cy5 fluorophore by chemical reaction with thiols

some reductants, such as ascorbic acid, to produce the non-fluorescent radical anions with tens of millisecond lifetimes under oxygen-depleted conditions [75, 78]. Since the photoswitching mechanism is relatively complex and depends on each fluorophore, the photoswitching ability is highly affected by the type of thiols/reductants, their concentrations, and the presence/absence of oxygen. Hence, considerable efforts are required to optimize the photoswitching property suitable for super-resolution imaging applications.

Moreover, the image quality in single-molecule localization-based super-resolution imaging is mainly affected by two properties, photon number and on–off duty cycle. The photon number refers to the detected photons in each cycle based on the absorption coefficient and fluorescence quantum yield of the fluorophores. As described in Eq. (3), the photon number is critical for resolution limit of the PSF in single-molecule detection. On the other hand, the on–off duty cycle is the dwell time of a fluorophore in the fluorescence "on" state. If the dwell time is too short, not enough photons can be detected during the acquisition time. However, if the dwell time is too long, precise detection of the positions of individual fluorophores would be difficult due to the increased probability of simultaneous emission in the diffraction-limited area. Therefore, high photon number and relatively low duty cycle are desired to obtain better super-resolution images. Dempsey et al. comprehensively evaluated the performance of a variety of organic fluorophores in terms of the properties of detectable photon numbers, on–off duty cycle, survival fraction, and number of switching cycles under STORM imaging conditions [79]. The latter two properties are related to photostability of the fluorophores. This study provided a better choice of fluorophores with excellent properties for STORM imaging (such as a Cy5 derivative Alexa647 and Dyomics654). They also demonstrated four-color STORM imaging by selecting suitable fluorophores without spectral overlap.

In contrast to the above dyes, photoswitchable dyes can be employed in single-molecule localization-based super-resolution microscopy without the addition of chemicals, such as thiols. Although several photochromic dyes based on azobenzenes, spiropyrans, and diarylethenes have light-induced reversible spectral change applicable to optical switches and memories [80], their application to single-molecule or super-resolution imaging has been rarely reported [81–84]. Rhodamine amides were known to have photochromic behaviors by nucleophilic addition of a deprotonated amide to the nine positions in a xanthene moiety upon photoirradiation which results in the formation of

a nonfluorescent spirolactamized isomer [85]. Three decades later, Fölling et al. developed a photochromic rhodamine B derivative substituted with 4-aminophthalimide at an amide position for single-molecule and subdiffraction imaging applications [86]. This molecule thermodynamically favors a nonfluorescent spirolactamized isomer in the dark state, while it converts to a fluorescent opened isomer upon UV irradiation. Since the open isomer spontaneously converts to the spirolactamized isomer, the number of activated fluorophores can be controlled by light irradiation without the help of external thiols. Photochromic dyes and their conjugates can perform reversible transitions between fluorescence "on" and "off" states in response to only photoirradiation. Although cellular imaging applications have currently remained challenging, such fluorophores would be available for super-resolution imaging without the need for optimization of the surrounding chemicals in the buffer.

Conclusions

In this mini-review, we summarize strategies to develop photostable and photoswitching fluorophores for super-resolution imaging. In these imaging methods, photostability is essential to acquire many photons from target objects with fluorophores to obtain subdiffraction images with good contrast. In particular, photostability is essential for STED microscopy that requires laser illumination with extremely high intensity. Since photobleaching occurs by chemical reactions in the triplet state of excited fluorophores, reducing the reactivity of the chromophore by chemical modifications, the use of triplet state quenchers is effective to elongate the emission duration. On the other hand, fluorescence switching by photoillumination is a key mechanism for single-molecule localization super-resolution microscopies, such as PALM and (d)STORM. Several photoactivatable fluorophores have been developed for PALM imaging by introducing photolabile groups into fluorophores. In addition, photoswitching properties of conventional fluorophores are extensively investigated in optimized conditions to realize (d)STORM imaging. Recently, subdiffraction imaging without photoswitching of fluorophores was demonstrated by single-molecule localization-based microscopy using spontaneously blinking fluorophores [87] or transiently binding fluorescent ligands [88–90]. However, photoswitching is still a versatile way to easily control the fluorescence by irradiation conditions. Further development of highly photostable and efficiently photoswitchable fluorophores would pave the way for super-resolution imaging applications, such as long-term live cell or in vivo imaging.

Labeling of organic fluorophores to target biomolecules is another issue. In contrast to fluorescent proteins, control of intracellular localization of organic fluorophores requires some techniques such as conjugation of fluorophores with ligands targeting specific biomolecules, such as cytoskeletons and nucleic acids [91, 92]. Conjugation methods by bio-orthogonal chemistry [93, 94] are also powerful tools for specifically tethering biomolecules with photostable or photoswitchable organic fluorophores for super-resolution imaging [95–98]. Labeling methods with expressed protein tags are also useful tools for imaging target proteins with the organic fluorophores in living cells. Several covalent and noncovalent tags have been reported [99–106], and some of them were applied to super-resolution imaging [107–112]. Furthermore, preparation techniques of objective samples by optical clearance and size expansion are becoming increasingly important for fluorescence imaging applications. Methods for optical clearing of tissues enabled wide 3D views of interactive cellular structures in tissues and whole body [113–115]. Size expansion of the imaging objects by polymer swelling after fixation can improve the resolution of optical microscopy, including super-resolution microscopy [116, 117]. Using the fluorophores in combination with labeling and preparation techniques, more detailed structures and dynamics of target biomolecules can be observed, which will reveal a novel biological function at a molecular level in living systems.

Acknowledgements This work was supported by Grants-in-Aid for Scientific Research of JSPS (Grants 25220207, 26102529, 15K12754 to K.K., and 16K01933 to M.M.), CREST of JST (K.K.), Asahi Glass Foundation (K.K.), Uehara Memorial Foundation (K.K.).

References

1. Chudakov DM, Matz MV, Lukyanov S, Lukyanov KA (2010) Fluorescent proteins and their applications in imaging living cells and tissues. Physiol Rev 90:1103–1163
2. Lavis LD, Raines RT (2014) Bright building blocks for chemical biology. ACS Chem Biol 9:855–866
3. Michalet X, Pinaud FF, Bentolila LA, Tsay JM, Doose S, Li JJ, Sundaresan G, Wu AM, Gambhir SS, Weiss S (2005) Quantum dots for live cells, in vivo imaging, and diagnostics. Science 307:538–544
4. Hell SW (2007) Far-field optical nanoscopy. Science 316:1153–1158
5. Huang B, Babcock H, Zhuang X (2010) Breaking the diffraction barrier: super-resolution imaging of cells. Cell 143:1047–1058
6. Abbe E (1873) Contributions to the understanding of microscope theory. Arch Mikrosk Anat 9:413–418
7. Hell SW, Wichmann J (1994) Breaking the diffraction resolution limit by stimulated emission: stimulated-emission-depletion fluorescence microscopy. Opt Lett 19:780–782
8. Klar TA, Jakobs S, Dyba M, Egner A, Hell SW (2000) Fluorescence microscopy with diffraction resolution barrier broken by stimulated emission. Proc Natl Acad Sci USA 97:8206–8210
9. Hofmann M, Eggeling C, Jakobs S, Hell SW (2005) Breaking the diffraction barrier in fluorescence microscopy at low light

intensities by using reversibly photoswitchable proteins. Proc Natl Acad Sci USA 102:17565–17569
10. Gustafsson MGL (2005) Nonlinear structured-illumination microscopy: wide-field fluorescence imaging with theoretically unlimited resolution. Proc Natl Acad Sci USA 102:13081–13086
11. Willig KI, Rizzoli SO, Westphal V, Jahn R, Hell SW (2006) STED microscopy reveals that synaptotagmin remains clustered after synaptic vesicle exocytosis. Nature 440:935–939
12. Willig KI, Kellner R, Medda R, Hein B, Jakobs S, Hell SW (2006) Nanoscale resolution in GFP-based microscopy. Nat Methods 3:721–723
13. Donnert G, Keller J, Medda R, Andrei MA, Rizzoli SO, Lührmann R, Jahn R, Eggeling C, Hell SW (2006) Macromolecular-scale resolution in biological fluorescence microscopy. Proc Natl Acad Sci USA 103:11440–11445
14. Eggeling C, Ringemann C, Medda R, Schwarzmann G, Sandhoff K, Polyakova S, Belov VN, Hein B, von Middendorff C, Schönle A (2009) Direct observation of the nanoscale dynamics of membrane lipids in a living cell. Nature 457:1159–1162
15. Westphal V, Rizzoli SO, Lauterbach MA, Kamin D, Jahn R, Hell SW (2008) Video-rate far-field optical nanoscopy dissects synaptic vesicle movement. Science 320:246–249
16. Nägerl UV, Willig KI, Hein B, Hell SW, Bonhoeffer T (2008) Live-cell imaging of dendritic spines by STED microscopy. Proc Natl Acad Sci USA 105:18982–18987
17. Schneider J, Zahn J, Maglione M, Sigrist SJ, Marquard J, Chojnacki, Kräusslich H-G, Sahl SJ, Engelhardt J, Hell SW (2015) Ultrafast, temporally stochastic STED nanoscopy of millisecond dynamics. Nat Methods 12:827–830
18. Berning S, Willig KI, Steffens H, Dibaj P, Hell SW (2012) Nanoscopy in a living mouse brain. Science 335:551
19. Gustaffson MGL (2000) Surpassing the lateral resolution limit by a factor of two using structured illumination microscopy. J Microsc 198:82–87
20. Schermelleh L, Carlton P, Haase S, Shao L, Winoto L, Kner P, Burke B, Cardoso CM, Agard DA, Gustafsson MGL, Leonhardt H, Sedat JW (2008) Subdiffraction multicolor imaging of the nuclear periphery with 3D structured illumination microscopy. Science 320:1332–1336
21. Kner P, Chhun B, Griffis E, Winoto L, Gustafsson MGL (2009) Super-resolution video microscopy of live cells by structured illumination. Nat Methods 6:339–342
22. Betzig E, Patterson GH, Sougrat R, Lindwasser OW, Olenych S, Bonifacino JS, Davidson MW, Lippincott-Schwartz, Hess HF (2006) Imaging intracellular fluorescent proteins at nanometer resolutio. Science 313:1642–1645
23. Rust MJ, Bates M, Zhuang X (2006) Sub-diffraction-limit imaging by stochastic optical reconstruction microscopy (STORM). Nat Methods 3:793–795
24. Betzig E, Trautman JK, Harris TD, Weiner JS, Kostelak RL (1991) Breaking the diffraction barrier-optical microscopy on a nanometric scale. Science 251:1468–1470
25. Axelrod D (1981) Cell-substrate contacts illuminated by total internal reflection fluorescence. J Cell Biol 89:141–145
26. Moerner WE (2006) Single-molecule mountains yield nanoscale cell images. Nat Methods 3:781–782
27. Shroff H, Galbraith CG, Galbraith JA, Betzig E (2008) Live-cell photoactivated localization microscopy of nanoscale adhesion dynamics. Nat Methods 5:417–423
28. Shim S-H, Xia C, Zhong G, Babcock HP, Vaughan JC, Huang B, Wnag X, Xu C, Bi G-Q, Zhuang X (2012) Super-resolution fluorescence imaging of organelles in live cells with photoswitchable membrane probes. Proc Acad Natl Sci USA 109:13978–13983
29. Kanchanawong P, Shtengel G, Pasapera A, Ramko E, Davidson M, Hess H, Waterman CM (2010) Nanoscale architecture of integrin-based cell adhesions. Nature 468:580–584
30. Bates M, Huang B, Dempsey GT, Zhuang X (2007) Multicolor super-resolution imaging with photo-switchable fluorescent probes. Science 317:1749–1753
31. Xu K, Zhong G, Zhuang X (2013) Actin, spectrin, and associated proteins form a periodic cytoskeletal structure in axons. Science 339:452–456
32. Chen KH, Boettiger AN, Moffitt JR, Wang S, Zhuang X (2015) Spatially resolved, highly multiplexed RNA profiling in single cell. Science 348:aaa6090
33. Boettiger AN, Bintu B, Moffitt JR, Wang S, Beliveau BJ, Fudenberg G, Imakaev M, Mirny LA, Wu CT, Zhuang X (2016) Super-resolution imaging reveals distinct chromatin folding for different epigenetic states. Nature 529(418):422
34. Jones SA, Shim S-H, He J, Zhuang X (2011) Fast, three-dimensional super-resolution imaging of live cells. Nat Methods 6:499–505
35. Hein B, Willig KI, Hell SW (2008) Stimulated emission depletion (STED) nanoscopy of a fluorescent protein-labeled organelle inside a living cell. Proc Natl Acad Sci USA 105:14271–14276
36. Kasche V, Lindqvist L (1964) Reactions between the triplet state of fluorescein and oxygen. J Phys Chem 68:817–823
37. Eggeling C, Widengren J, Rigler R, Seidel CAM (1998) Photobleaching of fluorescent dyes under conditions used for single-molecule detection: evidence of two-step photolysis. Anal Chem 70:2651–2659
38. Benesch RE, Benesch R (1953) Enzymatic removal of oxygen for polarography and related methods. Science 118:447–448
39. Mohanty J, Nau WM (2005) Host-guest complexation of neutral red with macrocyclic host molecules: Contrasting p*K*a shifts and binding affinities for cucurbit[7]uril and β-cyclodextrin. Angew Chem Int Ed 117:3816–3820
40. Martyn TA, Moor JL, Halterman RL, Yip WT (2007) Cucurbit[7]uril induces superior probe performance for single-molecule detection. J Am Chem Soc 129:10338–10339
41. Yau CM, Pascu SI, Odom SA, Warren JE, Klotz EJ, Frampton MJ, Williams CC, Coropceanu V, Kuimova MK, Phillips D, Barlow S, Brédas JL, Marder SR, Millar V, Anderson HL (2008) Stabilisation of a heptamethine cyanine dye by rotaxane encapsulation. Chem Commun (Camb) (25):2897–2899. doi:10.1039/b802728e
42. Yang SK, Shi X, Park S, Ha T, Zimmerman SC (2013) A dendritic single-molecule fluorescent probe that is monovalent, photostable and minimally blinking. Nat Chem 5:692–697
43. Komatsu T, Oushiki D, Takeda A, Miyamura M, Ueno T, Terai T, Nagano T (2011) Rational design of boron dipyrromethene (BODIPY)-based photobleaching-resistant fluorophores applicable to a protein dynamics study. Chem Commun 47:10055–10057
44. Toutchkine A, Nguyen D-V, Hahn KM (2007) Merocyanine dyes with improved photostability. Org Lett 9:2775–2777
45. Renikuntla BR, Rose HC, Eldo J, Waggoner AS, Armitage BA (2004) Improved photostability and fluorescence properties through polyfluorination of a cyanine dye. Org Lett 6:909–912
46. Panchuk-Voloshina N, Haugland RP, Bishop-Stewart J, Bhalgat MK, Millard PJ, Mao F, Leung W-Y, Haugland RP (1999) Alexa dyes, a series of new fluorescent dyes that yield exceptionally bright, photostable conjugates. J Histochem Cytochem 47:1179–1188
47. Grimm JB, English BP, Chen J, Slaughter JP, Zhang Z, Revyakin A, Patel R, Macklin JJ, Normanno D, Singer RH, Lionnet T, Lavis LD (2015) A general method to improve fluorophores

for live-cell and single-molecule microscopy. Nat Methods 12:244–250
48. Song X, Johnson A, Foley J (2008) 7-Azabicyclo [2.2.1] heptane as a unique and effective dialkylamino auxochrome moiety: demonstration in a fluorescent rhodamine dye. J Am Chem Soc 130:17652–17653
49. Song L, Varma CAGO, Verhoeven JW, Tanke HJ (1996) Influence of the triplet excited state on the photobleaching kinetics of fluorescein in microscopy. Biophys J 70:2959–2968
50. Giloh H, Sedat JW (1982) Fluorescence microscopy: reduced photobleaching of rhodamine and fluorescein protein conjugates by *n*-propyl gallate. Science 217:1252–1255
51. Widengren J, Chmyrov A, Eggeling C, Löfdahl PÅ, Seidel CA (2007) Strategies to improve photostabilities in ultrasensitive fluorescence spectroscopy. J Phys Chem A 111:429–440
52. Rasnik I, McKinney SA, Ha T (2006) Nonblinking and long-lasting single-molecule fluorescence imaging. Nat Methods 3:891–893
53. Cordes T, Vogelsang J, Tinnefeld P (2009) On the mechanism of Trolox as antiblinking and antibleaching reagent. J Am Chem Soc 131:5018–5019
54. Vogelsang J, Kasper R, Steinhauer C, Person B, Heilemann M, Sauer M, Tinnefeld P (2008) A reducing and oxidizing system minimizes photobleaching and blinking of fluorescent dyes. Angew Chem Int Ed 47:5465–5469
55. Adamczyk A, Wilkinson F (1972) Quenching of triplet states by Schiff base nickel (II) complexes. J Chem Soc, Faraday Trans 68:2031–2041
56. Glembockyte V, Lincoln R, Cosa G (2015) Cy3 photoprotection mediated by Ni^{2+} for extended single-molecule imaging: old tricks for new techniques. J Am Chem Soc 137:1116–1122
57. Altman RB, Terry DS, Zhou Z, Zheng Q, Geggier P, Kolster RA, Zhao Y, Javitch JA, Warren JD, Blanchard SC (2012) Cyanine fluorophore derivatives with enhanced photostability. Nat Methods 9:68–71
58. Altman RB, Zheng Q, Zhou Z, Terry DS, Warren JD, Blanchard SC (2012) Enhanced photostability of cyanine fluorophores across the visible spectrum. Nat Methods 9:428–429
59. Tinnefeld P, Cordes T (2012) Self-healing'dyes: intramolecular stabilization of organic fluorophores. Nat Methods 9:426–427
60. Zheng Q, Jockusch S, Zhou Z, Altman RB, Warren JD, Turro NJ, Blanchard SC (2012) On the mechanisms of cyanine fluorophore photostabilization. J Phys Chem Lett 3:2200–2203
61. van der Velde JHM, Oelerich J, Huang J, Smit JH, Jazi AA, Galiani S, Kolmakov K, Guoridis G, Eggeling C, Herrmann A, Roelfes G, Cordes T (2015) A simple and versatile design concept for fluorophore derivatives with intramolecular photostabilization. Nat Commun 7:10144
62. Grotjohann T, Testa I, Leutenegger M, Bock H, Urban NT, Lavoie-Cardinal F, Willig KI, Eggeling C, Jakobs S, Hell SW (2011) Diffraction-unlimited all-optical imaging and writing with a photochromic GFP. Nature 478:204–208
63. Brakemann T, Stiel AC, Weber G, Andresen M, Testa I, Grotjohann T, Leutenegger M, Plessmann U, Urlaub H, Eggeling C, Whal MC, Hell SW, Jakobs S (2011) A reversibly photoswitchable GFP-like protein with fluorescence excitation decoupled from switching. Nat Biotechnol 29:942–947
64. Grotjohann T, Testa I, Reuss M, Brakemann T, Eggeling C, Hell SW, Jakobs S (2012) rsEGFP2 enables fast RESOLFT nanoscopy of living cells. eLife 1:e00248
65. Tiwari DK, Arai Y, Yamanaka M, Matsuda T, Agetsuma M, Nakano M, Fujita K, Nagai T (2015) A fast-and positively photoswitchable fluorescent protein for ultralow-laser-power RESOLFT nanoscopy. Nat Methods 12:515–518
66. Adams SR, Tsien RY (1993) Controlling cell chemistry with caged compounds. Annu Rev Physiol 55:755–784
67. Klán P, Šolomek T, Bochet CG, Blanc A, Givens R, Rubina M, Popik V, Kostikov A, Wirz J (2013) Photoremovable protecting groups in chemistry and biology: reaction mechanisms and efficacy. Chem Rev 113:119–191
68. Mitchison TJ, Sawin KE, Theriot K, Mallavarapu GA (1998) Facile and general synthesis of photoactivatable xanthene dyes. Methods Enzymol 291:63–78
69. Wysocki L, Grimm J, Tkachuk A, Brown T, Betzig E, Lavis L (2011) Facile and general synthesis of photoactivatable xanthene dyes. Angew Chem Int Ed 50:11206–11209
70. Grimm J, Klein T, Kopek B, Shtengel G, Hess H, Sauer M, Lavis L, Grimm J, Klein T, Kopek B, Shtengel G, Hess H, Sauer M, Lavis L (2016) Synthesis of a Far-red photoactivatable silicon-containing rhodamine for super-resolution microscopy. Angew Chem Int Ed 55:1723–1727
71. Belov VN, Wurm CA, Boyarskiy VP, Jakobs S, Hell SW (2010) Rhodamines NN: a novel class of caged fluorescent dyes. Angew Chem Int Ed 49:3520–3523
72. Lord SJ, Conley NR, Lee HD, Samuel R, Liu N, Twieg RJ, Moerner WE (2008) A photoactivatable push–pull fluorophore for single-molecule imaging in live cells. J Am Chem Soc 130:9204–9205
73. Bates M, Blosser TR, Zhuang X (2005) Short-range spectroscopic ruler based on a single-molecule optical switch. Phys Rev Lett 94:108101
74. Heilemann M, van de Linde S, Schüttpelz M, Kasper R, Seefeldt B, Mukherjee A, Tinnefeld P, Sauer M (2008) Subdiffraction-resolution fluorescence imaging with conventional fluorescent probes. Angew Chem Int Ed 47:6172–6176
75. Heilemann M, van de Linde S, Mukherjee A, Sauer M (2009) Super-resolution imaging with small organic fluorophores. Angew Chem Int Ed 48:6903–6908
76. Vogelsang J, Cordes T, Forthmann C, Steinhauer C, Tinnefeld P (2009) Controlling the fluorescence of ordinary oxazine dyes for single-molecule switching and superresolution microscopy. Proc Natl Acad Sci USA 106:8107–8112
77. Dempsey GT, Bates M, Kowtoniuk WE, Liu DR, Tsien RY, Zhuang X (2009) Photoswitching mechanism of cyanine dyes. J Am Chem Soc 131:18192–18193
78. Heilemann M, Margeat E, Kasper R, Sauer M, Tinnefeld P (2005) Carbocyanine dyes as efficient reversible single-molecule optical switch. J Am Chem Soc 127:3801–3806
79. Dempsey GT, Vaughan JC, Chen KH, Bates M, Zhuang X (2011) Evaluation of fluorophores for optimal performance in localization-based super-resolution imaging. Nat Methods 8:1027–1036
80. Feringa BL, Browne WR (2011) Molecular switches, 2nd edn. Wiley-VCH, Weinheim
81. Bossi M, Belov V, Polyakova S, Hell SW (2006) Reversible red fluorescent molecular switches. Angew Chem Int Ed 45:7462–7465
82. Fukaminato T, Doi T, Tamaoki N, Okuno K, Ishibashi Y, Miyasaka H, Irie M (2011) Single-molecule fluorescence photoswitching of a diarylethene-perylenebisimide dyad: non-destructive fluorescence readout. J Am Chem Soc 133:4984–4990
83. Deniz E, Tomasulo M, Cusido J, Ylidiz I, Petriella M, Bossi ML, Sortino S, Raymo FM (2012) Photoactivatable fluorophores for super-resolution imaging based on oxazine auxochromes. J Phys Chem C 116:6058–6068
84. Pang S-C, Hyun H, Lee S, Jang D, Lee MJ, Kang SH, Ahn K-H (2012) Photoswitchable fluorescent diarylethene in a turn-on mode for live cell imaging. Chem Commun 48:3745–3747
85. Knauer KH, Gleiter R (1977) Photochromism of rhodamine derivatives. Angew Chem Int Ed 89:116–117
86. Fölling J, Belov V, Kunetsky R, Medda R, Schönle A, Egner A, Eggeling C, Bossi M, Hell SW (2007) Photochromic

rhodamines provide nanoscopy with optical sectioning. Angew Chem Int Ed 46:6266–6270
87. Uno S, Kamiya M, Yoshihara T, Sugawara K, Okabe K, Tarhan MC, Fujita H, Funatsu T, Okada Y, Tobita S, Urano Y (2014) A spontaneously blinking fluorophore based on intramolecular spirocyclization for live-cell super-resolution imaging. Nat Chem 6:681–689
88. Sharonov A, Hochstrasser R (2006) Wide-field subdiffraction imaging by accumulated binding of diffusing probes. Proc Natl Acad Sci USA 103:18911–18916
89. Jungmann R, Avendano MS, Woehrstein JB, Dai M, Shih WM, Yin P (2014) Multiplexed 3D cellular super-resolution imaging with DNA-PAINT and Exchange-PAINT. Nat Methods 11:313–318
90. Kiuchi T, Higuchi M, Takamura A, Maruoka M, Watanabe N (2015) Multitarget super-resolution microscopy with high-density labeling by exchangeable probes. Nat Methods 12:743–746
91. Lukinavičius G, Reymond L, D'Este E, Masharina A, Göttfert F, Ta H, Güther A, Fournier M, Rizzo S, Waldmann H, Blaukopf C, Sommer C, Gerlich DW, Arndt H-D, Hell SW, Johnsson K (2014) Fluorogenic probes for live-cell imaging of the cytoskeleton. Nat Methods 731:11–733
92. Lukinavičius G, Blaukopf C, Pershagen E, Schena A, Reymond L, Derivery E, Gonzalez-Gaitan M, D'Este E, Hell SW, Gerlich DW, Johnsson K (2015) SiR-Hoechst is a far-red DNA stain for live-cell nanoscopy. Nature Commun 6:8497
93. Best MD (2009) Click chemistry and bioorthogonal reactions: unprecedented selectivity in the labeling of biological molecules. Biochmistry 48:6571–6584
94. Hao Z, Hong S, Chen X, Chen PR (2011) Introducing bioorthogonal functionalities into proteins in living cells. Acc Chem Res 44:742–751
95. Zessin PJ, Finan K, Heilemann M (2012) Reversible fluorescence photoswitching in DNA. J Struct Biol 177:344–348
96. Letschert S, Göhler A, Franke C, Bertleff-Zieschang N, Memmel E, Doose S, Seibel J, Sauer M (2014) Super-resolution imaging of plasma membrane glycans. Angew Chem Int Ed 53:10921–10924
97. Nikić I, Plass T, Schraidt O, Szymański J, Briggs JA, Schultz C, Lemke EA (2014) Live-cell imaging of cyclopropene tags with fluorogenic tetrazine cycloadditions. Angew Chem Int Ed 53:2245–2249
98. Uttamapinant C, Howe JD, Lang K, Beránek V, Davis L, Mahesh M, Barry NP, Chin JW (2015) Genetic code expansion enables live-cell and super-resolution imaging of site-specifically labeled cellular proteins. J Am Chem Soc 137:4602–4605
99. Griffin BA, Adams SR, Tsien RY (1998) Specific covalent labeling of recombinant protein molecules inside live cells. Science 281:269–272
100. Los GV, Encell LP, McDougall MG, Hartzell DD, Karassina N, Zimprich C, Wood MG, Learish R, Ohana RF, Urh M, Simpson D, Mendez J, Zimmerman K, Otto P, Vidugiris G, Zhu J, Darzins A, Klaubert DH, Bulleit RF, Wood KV (2008) HaloTag: a novel protein labeling technology for cell imaging and protein analysis. ACS Chem Biol 3:373–382
101. Keppler A, Gendreizig S, Gronemeyer T, Pick H, Vogel H, Johnsson K (2003) A general method for the covalent labeling of fusion proteins with small molecules in vivo. Nat Biotechnol 21:86–89
102. Miller LW, Sable J, Goelet P, Sheetz MP, Cornish VW (2004) Methotrexate conjugates: a molecular in vivo protein tag. Angew Chem Int Ed 116:1704–1707
103. Mizukami S, Watanabe S, Hori Y, Kikuchi K (2009) Covalent protein labeling based on noncatalytic β-lactamase and a designed FRET substrate. J Am Chem Soc 131:5016–5017
104. Hori Y, Nakaki K, Sato M, Mizukami S, Kikuchi K (2012) Development of protein-labeling probes with a redesigned fluorogenic switch based on intramolecular association for no-wash live-cell imaging. Angew Chem Int Ed 51:5611–5614
105. Szent-Gyorgyi C, Schmidt BF, Creeger Y, Fisher GW, Zakel KL, Adler S, Fitzpatrick AJ, Woolford CA, Yan Q, Vasilev KV, Berget PB, Bruchez MP, Jarvic JW, Waggoner A (2008) Fluorogen-activating single-chain antibodies for imaging cell surface proteins. Nat Biotechnol 26:235–240
106. Chen I, Howarth M, Lin W, Ting AY (2005) Site-specific labeling of cell surface proteins with biophysical probes using biotin ligase. Nat Methods 2:99–104
107. Lee HD, Lord SJ, Iwanaga S, Zhan K, Xie H, Williams JC, Wang H, Bowman GR, Goley ED, Shapiro L, Twieg RJ, Rao J, Moerner WE (2010) Superresolution imaging of targeted proteins in fixed and living cells using photoactivatable organic fluorophores. J Am Chem Soc 132:15099–15101
108. Lelek M, Di Nunzio F, Henriques R, Charneau P, Arhel N, Zimmer C (2012) Superresolution imaging of HIV in infected cells with FlAsH-PALM. Proc Natl Acad Sci USA 109:8564–8569
109. Wilmes S, Staufenbiel M, Liße D, Richter CP, Beutel O, Busch KB, Hess ST, Piehler J (2012) Triple-color super-resolution imaging of live cells: resolving submicroscopic receptor organization in the plasma membrane. Angew Chem Int Ed 51:4868–4871
110. Lukinavičius G, Umezawa K, Olivier N, Honigmann A, Yang G, Plass T, Mueller V, Reymond L, Correa I Jr, Luo Z-G, Schultz C, Lemke EA, Heppenstall P, Eggeling C, Manley S, Johnsson K (2013) A near-infrared fluorophore for live-cell super-resolution microscopy of cellular proteins. Nat Chem 5:132–139
111. Wombacher R, Heidbreder M, van de Linde S, Sheetz MP, Heilemann M, Cornish VW, Sauer M (2010) Live-cell super-resolution imaging with trimethoprim conjugates. Nat Methods 7:717–719
112. Fitzpatrick JAJ, Yan Q, Sieber JJ, Dyba M, Schwarz U, Szent-Gyorgyi C, Woolford CA, Berget PB, Waggoner AS, Bruchez MP (2009) STED nanoscopy in living cells using fluorogen activating proteins. Bioconjugate Chem 20:1843–1847
113. Hama H, Kurokawa H, Kawano H, Ando R, Shimogori T, Noda H, Fukami K, Sakaue-Sawano A, Miyawaki A (2011) Scale: a chemical approach for fluorescence imaging and reconstruction of transparent mouse brain. Nat Neurosci 14:1481–1488
114. Chung K, Wallace J, Kim SY, Kalyanasundaram S, Andalman AS, Davidson TJ, Mirzabekov JJ, Zalocusky KA, Mattis J, Denisin AK, Pak S, Bernstein H, Ramakrishnan C, Grosenick L, Gradinaru V, Deisseroth K (2013) Structural and molecular interrogation of intact biological systems. Nature 497:332–337
115. Susaki EA, Tainaka K, Perrin D, Kishino F, Tawara T, Watanabe TM, Yokoyama C, Onoe H, Eguchi M, Yamaguchi S, Abe T, Kiyonari H, Shimizu Y, Miyawaki A, Yokota H, Ueda HR (2014) Whole-brain imaging with single-cell resolution using chemical cocktails and computational analysis. Cell 157:726–739
116. Chen F, Tillberg PW, Boyden ES (2015) Expansion microscopy. Science 347:543–548
117. Chozinski TJ, Halpern AR, Okawa H, Kim HJ, Tremel GJ, Wong RO, Vaughan JC (2016) Expansion microscopy with conventional antibodies and fluorescent proteins. Nat Methods 13:485–488